Journal of Petroleum Exploration and Production Technology
https://doi.org/10.1007/s13202-024-01785-9

ORIGINAL PAPER-EXPLORATION ENGINEERING

Multi-objective optimization of parameters design based on genetic algorithm in annulus aerated dual gradient drilling

Qian Li[1] · Xiaolin Zhang[1] · Hu Yin[1]

Received: 19 October 2023 / Accepted: 7 March 2024

Abstract

The optimization of drilling parameters is crucial for resolving the drilling problems in low-pressure and leaky formations using the annulus aerated dual gradient drilling technology. However, the previous studies have mostly focused on engineering applications and wellbore fluid flow models, with less emphasis on parameter optimization. This paper combines the wellbore multiphase flow model with genetic algorithms for the first time, proposing a key parameter optimization method for annulus aerated dual gradient drilling based on genetic algorithms. The study investigates the impact of selection operators on the performance of genetic algorithms and compares genetic algorithms with PSO algorithm and SAA. The results indicate that the convergence and stability of genetic algorithms can be improved by enhancing the selection operators. Compared to the gas–liquid ratio parameter optimization method, the IRSGA optimization method reduces the cost coefficient by 36.46%. Through comparative analysis of different optimization methods, the IRSGA demonstrates over 95% accuracy in large-scale computations. The research findings contribute to the optimization of parameters design under low-cost conditions and are of significant importance for promoting the use of this technology to address the serious issue of lost circulation in drilling technology.

Keywords Genetic algorithm · Annulus aerated · Multiphase flow · Dual gradient · Multi-objective optimization

List of symbols

A	Cross-sectional area of wellbore annulus, m^2
A_i	The i-th generation population in optimization algorithm
a_i	The i-th individual in the population
C_{air}	Daily expenses of one air compressor, \$/d
C_{ddp}	Daily rental cost of one dual-wall drill pipe, \$/d
C_h	Daily cost of the wellhead back pressure equipment, \$/d
C_l	Daily cost of one drilling fluid pump, \$/d
C_{pg}	Specific heat of gas, J/(kg·◦C)
C_{pl}	Specific heat of liquid, J/(kg·◦C)
E_g	Void fraction of wellbore annulus section, dimensionless
E_l	Liquid fraction of wellbore annulus section, dimensionless
E_s	Cuttings fraction of wellbore annulus section, dimensionless
F_r	Annulus friction pressure drop, Pa
g	Gravitational acceleration, m/s^2
H_g	Depth of the gas injection point, m
H_{g0}	Length of one dual-wall drill pipe, m
H_{g1}	Estimated drilling footage of the drill trip, m
m_g	Mass flow rate of gas phase, kg/s
m_l	Mass flow rate of liquid phase, kg/s
N	The size of population
P	Annulus pressure, Pa
P_{atm}	The standard atmospheric pressure, Pa
P_{calc}	Model calculation pressure at measuring point, MPa
P_f	Formation fracture pressure, Pa
P_h	Wellhead back pressure, Pa
$P_{off\text{-}line}$	The off-line performance
$P_{on\text{-}line}$	The on-line performance
P_p	Formation pore pressure, Pa
P_{safe}	Bottom-hole safety factor, dimensionless
P_{test}	Test pressure at measuring point, MPa
Q_g	Aerated rate of gas under standard conditions, m^3/s

✉ Xiaolin Zhang
997642790@qq.com

[1] Petroleum Engineering School, Southwest Petroleum University, Chengdu 610500, China

Published online: 08 April 2024

Q_{g0}	Maximum displacement of one air compressor, m^3/s
Q_l	Flow rate of the drilling fluid, m^3/s
Q_{l0}	Maximum displacement of one drilling fluid pump, m^3/s
q_g	Mass rate of aerated gas at the injection point, kg/(s·m)
R_e	Relative error
T	Maximum number of iterations
T_a	Temperature in annulus, ◦C
T_f	Temperature in formation, ◦C
T_p	Temperature in drill pipe, ◦C
v_g	Velocity of the aerated gas in the wellbore annulus, m/s
v_l	Velocity of drilling fluid, m/s
v_s	Velocity of cuttings, m/s
X'	Heat transfer factor between formation and annulus fluid, ◦C·m·s/J
Y'	Heat transfer factor between annulus fluid and drill string fluid, ◦C·m·s/J
θ	Well deviation angle, °
ρ_g	Density of gas under the condition of wellbore temperature and pressure, kg/m^3
ρ_l	Density of drilling fluid, kg/m^3
ρ_s	Density of cuttings, kg/m^3

Abbreviations

AR	The accuracy rate
$C\_Fitness_i$	Sum of fitness values for the i individuals in contemporary generation
GA	Genetic algorithm
Gap	Generation gap
GC	Global convergence
IRSGA	Improved roulette selection operator genetic algorithm
LC	Local convergence
MWD	Measurement while drilling
ORSGA	Original roulette selection operator genetic algorithm
P_Cross	Crossover probability
P_Mutate	Mutation probability
PSO	Particle swarm optimization
RSGA	Ranking selection operator genetic algorithm
SAA	Simulated annealing algorithm
TSGA	Tournament selection operator genetic algorithm

Introduction

Lost circulation is one of the inevitable problems in drilling engineering, causing economic losses of billions of dollars annually (Sun et al. 2021). In order to address the safe drilling issues in formations with narrow pressure windows or lost circulation formations, numerous experts and scholars have proposed unconventional drilling techniques, among which dual gradient drilling technology is one (Stave et al. 2014; Yang et al. 2022). Currently, offshore dual gradient drilling technology is developing rapidly and has certain commercial application value. Offshore dual gradient drilling technology includes lifting drilling fluid through subsea mud pumps, riserless drilling, and dual-density drilling. Onshore, due to limited underground space and cost constraints, dual gradient drilling technology development is relatively lagging. It typically achieves dual gradient drilling through gas injection. Commonly used onshore dual gradient drilling technologies include parasitic pipe gas injection and concentric pipe gas injection drilling technology (Dou et al. 2013; Gonzalez et al. 2013).

Phillips Petroleum Company conducted a parasitic annulus air-injection drilling test in Gallatin County, Montana (Westermark 1986). By injecting air into the annulus space through a parasitic air-injection pipe and setting the appropriate air/mud ratio and depth of air injection, the equivalent density of bottom-hole pressure could be reduced to 0.719. Guo and Rajtar (1995) proposed a simple method to calculate the ratio of drilling fluid to gas for aerated drilling, which can be used for bottom-hole pressure calculations. Lopes and Bourgoyne (1997) developed a steady-state numerical model to calculate parameters such as gas injection rate, maximum drilling fluid density, and riser diameter for gas injection dual gradient drilling in deep water. Li (2007) systematically described the process flow, equipment, application scope, and development direction of the low-pressure drilling technology with dual-wall drill pipe. Zimuzor et al. (2010) used gas injection drilling with parasitic pipe to solve wellbore leakage and stuck pipe problems in the Piceance Basin. This technology controlled the annulus circulating density by injecting air through a parasitic pipe in annulus, successfully reducing the risk of wellbore leakage in the Piceance Basin. Dou et al. (2013) referenced the Hasan-Kabir model (1986) to analyze the influence of gas injection rate and back pressure at the wellhead on bottom-hole pressure in annulus air-injection drilling with parasitic pipe. It was found that as the gas injection rate increased, the bottom-hole pressure initially decreased rapidly and then slowly increased, indicating the existence of a critical gas injection rate. Ma et al. (2014) simulated the temperature distribution in the riser of gas injection dual gradient drilling. The results showed that an increase in the inlet temperature correspondingly increased the temperature in the annulus. Su et al. (2018) studied the physical process of gas migration in the riser of gas injection dual gradient drilling. The research results showed that a high drilling fluid flow rate could eliminate large bubbles and stabilize wellbore pressure. Wang et al. (2019) designed a new deepwater dual

gradient drilling method based on downhole separation. The research results showed that optimizing the wellbore pressure profile could adapt to narrower pressure window and effectively avoid complex downhole accidents caused by improper wellbore pressure.

In summary, the previous research on the construction parameters of annular gas injection dual gradient drilling has mainly focused on engineering applications, wellbore fluid modeling, and drilling parameter design. Parameter design optimization is usually based on empirical formulas. There has been limited research on optimizing construction parameters, and the optimization objectives have been single-focused, considering only wellbore pressure safety without taking cost into account. Therefore, further research is needed to establish a method for optimizing construction parameters for annular gas injection dual gradient drilling that simultaneously considers cost and wellbore safety conditions. This will provide theoretical support for the promotion of this technology to address severe wellbore leakage in drilling operations.

This paper presents an onshore dual gradient drilling using dual-wall drill pipes for annulus gas injection. The process flow is shown in Fig. 1. This technique regulates the bottom-hole pressure through control of drilling fluid displacement, gas injection rate, gas injection depth, and wellhead back pressure. Compared to the aerated mud drilling: (1) It effectively avoids the impact of gas on screw drill tools and MWD; (2) as the gas injection depth is relatively shallower, the gas injection pressure is lower; and (3) gas injection into the casing helps prevent erosion on the mud cake, thereby promoting wellbore stability. In comparison with aerated drilling with a parasitic pipe, it eliminates the issues associated with parasitic pipe blockage, as well as the challenges of repairing and replacing the pipe. GA (Chande and Sinha 2013) is an optimization algorithm based on the principles of biological evolution. Its basic idea is to simulate the processes of natural selection, genetic variation, and mutation in biological evolution to search and optimize the solution space. The advantages of GA lie in their wide applicability, strong parallel processing capabilities, independence from constraints and differentiability, robustness, and global search ability (Ong et al. 2019). GA can be particularly useful when the search space is large and the objective function is not well-behaved or has multiple local optima. In this study, a genetic algorithm is employed, with drilling fluid displacement, gas injection rate, gas injection depth, and wellhead back pressure as decision variables, and the safety of bottom-hole pressure and construction cost as objective functions for multi-objective optimization. It provides an optimal combination of parameters with low cost, laying a foundation for applying this technology to solve drilling problems in severely lost circulation formations.

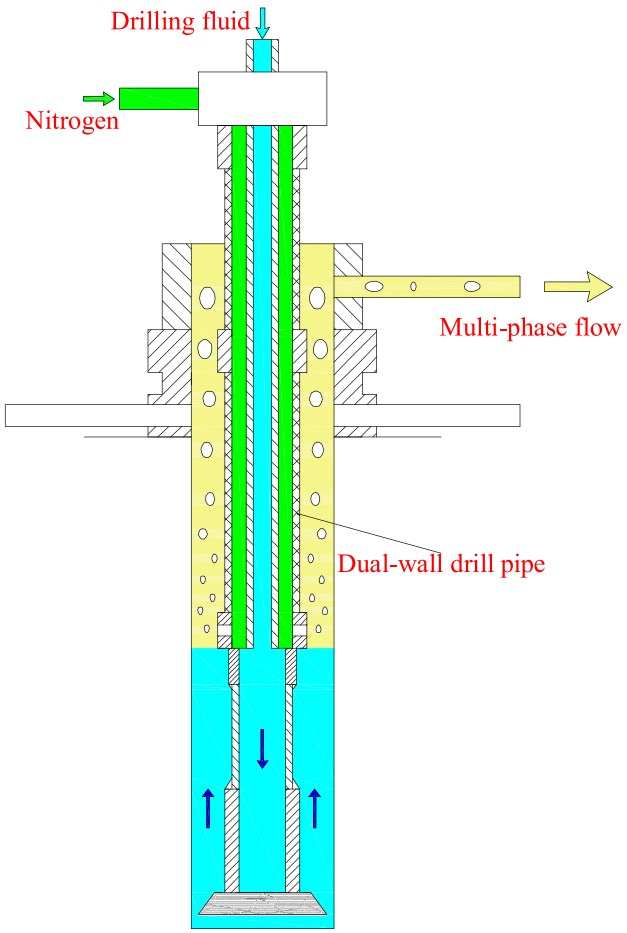

Fig. 1 Schematic diagram of annulus aerated dual gradient drilling with dual-wall drill pipe

In response to the issues of using empirical formulas to optimize parameters, limited optimization methods, and single optimization objectives in the previous studies on annulus aerated dual gradient drilling, this study has developed a multi-objective optimization method for parameters. The gaps addressed in this study include the following areas:

1) For the first time, a multi-objective optimization method based on genetic algorithm for parameters of annulus aerated dual gradient drilling was established with the objectives of wellbore safety and construction cost.
2) The impact of different selection operators on genetic algorithm was analyzed, and the efficiency of the optimization method could be further enhanced by improving the selection operator.
3) Several algorithms were compared to evaluate the parameter optimization algorithm in terms of effectiveness, efficiency, and accuracy for algorithm improvement.

Multiphase flow model for annulus aerated dual gradient drilling

Assumption

1) Fluid is a continuous infinitesimal material system, and the pressure and flow velocity of the fluid vary continuously.
2) Drilling fluid is an incompressible fluid.
3) The fluid flows axially along the wellbore in one-dimensional direction.

Continuity equation

Take the microelement along the axial direction of the annulus space to form a control volume (Meng et al. 2015). Analyze the components flowing into and out of the control volume per unit time:

(1) Gas phase

$$\frac{\partial\left(\rho_g v_g A E_g\right)}{\partial z}+\frac{\partial\left(\rho_g A E_g\right)}{\partial t}=q_g \tag{1}$$

(2) Liquid phase

$$\frac{\partial\left(\rho_l v_l A E_l\right)}{\partial z}+\frac{\partial\left(\rho_l A E_l\right)}{\partial t}=0 \tag{2}$$

(3) Cuttings phase

$$\frac{\partial\left(\rho_s v_s A E_s\right)}{\partial z}+\frac{\partial\left(\rho_s A E_s\right)}{\partial t}=0 \tag{3}$$

where ρ_g is the density of gas under the condition of wellbore temperature and pressure, kg/m^3; v_g is the velocity of the aerated gas in the wellbore annulus, m/s; A is the cross-sectional area of wellbore annulus, m^2; E_g is the void fraction of wellbore annulus section, dimensionless; q_g is the mass rate of aerated gas at the injection point, kg/(s·m), and $q_g=0$ if there is no gas injection point in the control element; ρ_l is the density of drilling fluid, kg/m^3; v_l is the velocity of drilling fluid, m/s; E_l is the liquid fraction of wellbore annulus section, dimensionless; ρ_s is the density of cuttings, kg/m^3; v_s is the velocity of cuttings, m/s; and E_s is the cuttings fraction of wellbore annulus section, dimensionless.

Momentum equation

The force analysis of the annulus microelement control body is shown in Fig. 2. According to the law of momentum, the momentum equation of gas, liquid, and solid three-phase flow can be written as follows:

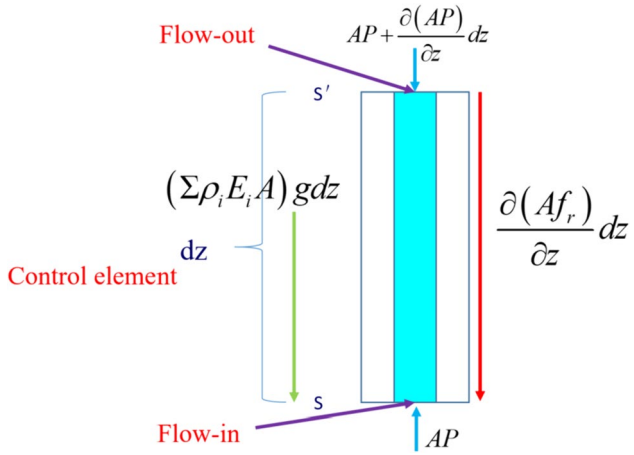

Fig. 2 Force analysis of the annulus microelement control body

$$\begin{aligned}&\frac{\partial}{\partial t}\left(AE_g\rho_g v_g+AE_l\rho_l v_l+AE_s\rho_s v_s\right)+\frac{\partial}{\partial z}\left(AE_g\rho_g v_g^2+AE_l\rho_l v_l^2+AE_s\rho_s v_s^2\right)\\&+Ag\cos\theta\left(\rho_g E_g+\rho_l E_l+\rho_s E_s\right)\Sigma+\frac{\partial(AP)}{\partial z}+\frac{\partial\left(AF_r\right)}{\partial z}=0\end{aligned} \tag{4}$$

where g is gravitational acceleration, m/s^2; θ is the well deviation angle, °; P is annulus pressure, Pa; and F_r is the annulus friction pressure drop, Pa.

Energy equation

Compared with non-gas injection drilling, the wellbore heat exchange of gas injection drilling becomes more complex. There is not only heat exchange between the formation and the wellbore fluid, but also heat exchange caused by the gas in the annulus. Therefore, the energy equation for the annulus multiphase can be expressed as follows:

$$\begin{aligned}&\frac{\partial}{\partial t}\left(\rho_g E_g C_{pg} T_a A+\rho_l E_l C_{pl} T_a A\right)-\frac{\partial}{\partial z}\left(m_g C_{pg} T_a+m_l C_{pl} T_a\right)\\&=\frac{2}{X'}\left(T_f-T_a\right)-\frac{2}{Y'}\left(T_a-T_p\right)\end{aligned} \tag{5}$$

where C_{pg} and C_{pl} are the specific heat of gas and liquid, respectively, J/(kg·◦C); T_a, T_f, and T_p are the temperature in annulus, formation, and drill pipe, ◦C; m_g and m_l are mass flow rate of gas phase and liquid phase, kg/s; X' is the comprehensive heat transfer factor between formation and annulus fluid, ◦C·m·s/J; and Y' is the heat transfer factor between annulus fluid and drill string fluid, ◦C·m·s/J.

Optimization of parameters design for annulus aerated dual gradient drilling based on genetic algorithm

Formulation of the optimization problem

In the issue of parameters optimization for annulus aerated dual gradient drilling, the most important objective is to ensure the safety of the bottom-hole pressure through parameter combination while minimizing drilling costs as much as possible.

Decision variables

In the multi-objective optimization problem mentioned above, decision variables include drilling fluid displacement, gas injection rate, gas injection depth, and wellhead back pressure.

Objective functions (1) The first objective function is the bottom-hole safety factor:

$$P_{\text{safe}}\left(Q_l, Q_g, H_g, P_h\right) = \frac{\left|P\left(Q_l, Q_g, H_g, P_h\right) - \left(P_p + \frac{(P_f - P_p)}{2}\right)\right|}{P_p + \frac{(P_f - P_p)}{2}} \tag{6}$$

where P_{safe} is the bottom-hole safety factor, dimensionless; P_p is the formation pore pressure, Pa; Q_l is the flow rate of drilling fluid, m^3/s; Q_g is the injection rate of aerated gas under standard conditions, m^3/s; H_g is the depth of gas injection point, m; P_h is the wellhead back pressure, Pa; P_f is the formation fracture pressure, Pa; and P is the bottom-hole pressure under specific parameter combination, Pa.

Assuming that $P = P_f$, the bottom-hole safety factor becomes the maximum value, represented by P^*_{safe}:

$$P^*_{\text{safe}} = \frac{\left|P_f - P_p\right|}{P_f + P_p} \tag{7}$$

According to Eqs.(6) and (7), it is obvious that the smaller the P_{safe} value is, the higher the safety of the well bore would be.

(2) The second objective function is the cost index:

$$C_{\cos t}\left(Q_l, Q_g, H_g, P_h\right) = \left(\left\lfloor \frac{Q_l}{Q_{l0}} \right\rfloor + 1\right) \times C_l + \left(\left\lfloor \frac{Q_g}{Q_{g0}} \right\rfloor + 1\right) \times C_{\text{air}} + \left(\left\lfloor \frac{H_g + H_{g1}}{H_{g0}} \right\rfloor + 1\right) \times C_{\text{ddp}} + \frac{P_h}{P_{\text{atm}}} \times C_h \tag{8}$$

where C_l is the daily cost of one drilling fluid pump, \$/d; C_{air} is the daily expenses of one air compressor, \$/d; Q_{l0} is the maximum displacement of one drilling fluid pump, m^3/s; Q_{g0} is the maximum displacement of one air compressor, m^3/s; H_{g0} is the length of one dual-wall drill pipe, m; H_{g1} is the estimated drilling footage of the drill trip, m; C_{ddp} is the daily rental cost of one dual-wall drill pipe, \$/d; P_{atm} is the standard atmospheric pressure, Pa; and C_h is the daily usage cost of the wellhead back pressure equipment, \$/d.

Constraints

There are some constraints that limit the search space in the considered optimization problem.

(1) The allowed ranges of drilling fluid displacement:

$$Q_{l\min} \le Q_l \le Q_{l\max} \tag{9}$$

The minimum drilling fluid displacement is determined by meeting the minimum requirement for borehole cuttings transport, while the maximum drilling fluid displacement is determined by the capacity of the drilling fluid pumps.

(2) The allowed ranges of gas injection rate:

$$Q_{g\min} \le Q_g \le Q_{g\max} \tag{10}$$

The minimum and maximum values of the gas injection velocity are determined by the air compressor.

(3) The limit depths of gas injection point:

$$H_{g\min} \le H_g \le H_{g\max} \tag{11}$$

The minimum depth for gas injection is the length of a dual-wall drill pipe, while the maximum injection depth is determined by the maximum gas injection pressure provided by the air compressor.

(4) Wellhead back pressure:

$$P_{h\min} \le P_h \le P_{h\max} \tag{12}$$

The minimum wellhead back pressure is atmospheric pressure, while the maximum value is determined by the capacity of the throttle valve.

IRSGA for parameters optimization

The traditional methods make it difficult to perform comprehensive constrained optimization of parameters design for annulus aerated dual gradient drilling. In this paper, an improved genetic algorithm is proposed for multi-objective optimization of parameters design for annulus aerated dual gradient drilling.

Initialization of population

Each individual consists of four gene segments, with each gene segment representing a different decision variable. A

certain number of individuals are randomly generated as the initial population, with each individual representing a potential solution to the optimization problem. Based on the form of the objective function, the population individuals can be defined as follows:

$$a_i = \left[Q_{il}, Q_{ig}, H_{ig}, P_{ih}\right] \tag{13}$$

The size of population is represented by N; therefore, the first population is A_1:

$$A_1 = \left[a_1, a_2, \ldots a_i \ldots a_{N-1}, a_N\right]^{\mathrm{T}} \tag{14}$$

Fitness value

According to Eqs.(6) and (8), the fitness value is expressed as follows:

$$\mathrm{Fitness}_i = \frac{1}{e^{P_{\mathrm{safe}}\left(Q_{il}, Q_{ig}, H_{ig}, P_{ih}\right)}} \times w_1 + \frac{1}{e^{C_{\cos t}\left(Q_{il}, Q_{ig}, H_{ig}, P_{ih}\right)}} \times w_2 \tag{15}$$

where w_1 and w_2 are weight coefficient. And $w_1 + w_2 = 1$.

The higher the fitness value, the better the individual in the population, and the more likely it is to be selected by the selection operator.

The sum of fitness values for the i individuals in contemporary generation is defined as $C\_Fitness_i$:

$$C\_\mathrm{Fitness}_i = C\_\mathrm{Fitness}_{i-1} + \mathrm{Fitness}_i \tag{16}$$

$$C\_\mathrm{Fitness}_N = \sum_{1}^{N} \mathrm{Fitness}_i \tag{17}$$

Selection operator

The selection operator in genetic algorithm selects a portion of individuals from the current population as parents for the next generation according to their fitness evaluation values. Common selection operators include roulette wheel selection, tournament selection, and rank selection (Mao et al. 2020; Pandey 2016). Original roulette wheel selection selects only one parent individual at a time, which may result in better individuals being selected too much and accelerating convergence, or poorer individuals being selected too much and reducing evolutionary efficiency. In this paper, an improved roulette wheel selection operator is proposed, which selects multiple parent individuals at a time for crossover and mutation operations. This approach helps introduce more genetic information and diversity, and enhances the algorithm's exploration capability.

Steps for the improved roulette selection operator are as follows:

① Firstly, let $M = C\_Fitness_N / N_{select}$, and randomly generate a real number $RX (RX \in [0, M])$;

② Secondly, let $j=1 (j \in [1, N_{select}])$, $i=1 (i \in [1, N])$, $b_0=0$ and $C\_Fitness_0=0$;

③ Thirdly, define $b_j = RX + (j\text{-}1) \times M$;

④ Determine whether $b_j\text{-}1 < fitness_i \le b_j$ is valid;

⑤ If step ④ is false, let $i = i + 1$, and turn to step ④;

⑥ If step ④ is true, a_i is selected as a parent individual. Then, let $i = i + 1$, $j = j + 1$, and jump to step ③. Loop until N_{select} parent individuals are selected.

Cross recombination

To ensure the diversity of the population and improve the global search capability, the N_{select} parent individuals are subjected to crossover operations:

① Choose two individuals, denoted as a_1 and a_2, from the N_{select} parent individuals. Randomly generate a real number $RX (RX \in [0, C\_Fitness_N])$. If $RX > P\_Cross$, $b_1 = a_1$ and $b_2 = a_2$. Turn to step ④.

② If $RX \le P\_Cross$, a_1 and a_2 perform cross recombination. The parent individuals a_1 and a_2 are scaled by removing the decimal point, resulting in c_1 and c_2. Binary encoding is then applied to c_1 and c_2, producing binary gene fragments d_1 and d_2. A random crossover point within the gene fragments is selected. The gene fragment preceding the crossover point in d_1 and the gene fragment following the same crossover point in d_2 are copied to create the offspring individual e_1;

③ Similarly, the gene fragment following the same crossover point in d_1 and the gene fragment preceding the crossover point in d_2 are copied to create the offspring individual e_2. Decimal encoding is then applied to e_1 and e_2, resulting in f_1 and f_2. Finally, f_1 and f_2 are scaled to obtain the new offspring individuals b_1 and b_2. As depicted in Fig. 3, two new offspring individuals, b_1 and b_2, are created, inheriting the genetic traits of their respective parents.

④ Repeat the steps ①–③ until all the N_{select} parent individuals are executed.

Where P_Cross is the probability of cross recombination.

Table 1 illustrates an example of the cross recombination operation. The parent individuals a_1 and a_2 consist of four gene fragments, representing drilling fluid displacement, gas injection rate, gas injection depth, and wellhead back pressure. The specific steps are as follows: (1) Scale the parent individuals a_1 and a_2 by removing the decimal point, resulting in c_1 and c_2. (2) Perform binary encoding on the gene fragments of c_1 and c_2, obtaining d_1 and d_2. The length of each gene segment is determined by the maximum value of the corresponding parameter during the encoding process. The maximum values of the parameters are presented in Table 3. The binary encoding lengths for each gene segment are 11, 13, 18, and 7, respectively. If the length of

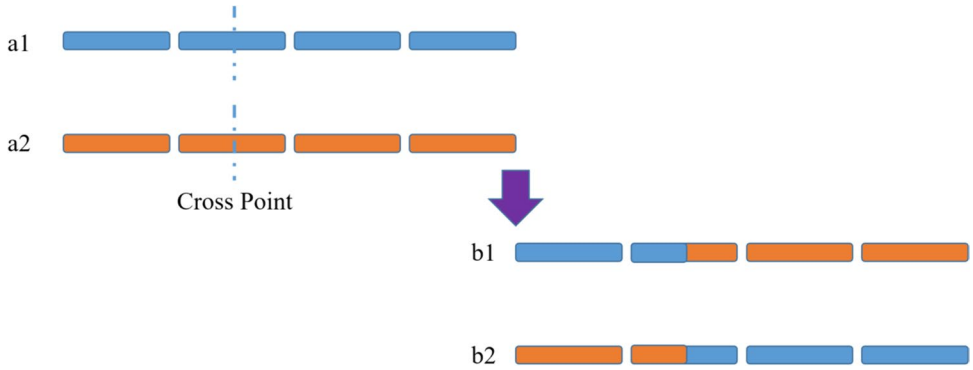

Fig. 3 Schematic diagram of cross recombination

Table 1 Example of cross recombination

Operation	Individual	Drilling fluid displacement	Gas injection rate	Gas injection depth	Wellhead back pressure
/	a_1	13.11	65.21	2315.79	0.34
	a_2	6.98	34.89	472.06	0.69
Scale	c_1	1311	6521	231,579	34
	c_2	698	3489	47,206	69
Binary encode	d_1	10,100,011,111	1,100,101,111,001	111,000,100,010,011,000	0100010
	d_2	01010111010	0110110100001	001011100001100110	1,000,101
Cross	e_1	01010111010	0110110100001	001011100010011000	0100010
	e_2	10,100,011,111	1,100,101,111,001	111,000,100,001,100,110	1,000,101
Decimal code	f_1	698	3489	47,256	34
	f_2	1311	6521	231,526	69
Scale	b_1	6.98	34.89	472.56	0.34
	b_2	13.11	65.21	2315.26	0.69

the converted binary gene segment is insufficient, it will be padded with zeros. (3) A cross point is randomly selected. In this example, the total length of the parent gene is 49, and the cross point is set at 30. The gene fragments in the parent individuals d_1 and d_2 are exchanged to generate binary offspring e_1 and e_2. (4) The binary offspring e_1 and e_2 are decoded to obtain f_1 and f_2. Finally, the target offspring b_1 and b_2 are obtained by scaling f_1 and f_2. If any of the parameters in the target offspring exceed the extreme value, the extreme value will be used instead.

Mutation

In order to further enhance the exploration ability of solution space, mutation operations are performed on N_{select} populations generated through crossover operations to introduce new gene disturbances:

① For each parent individual in the selected population N_{select}, generate a random real number RX ($RX \in [0,1]$). If $RX > P\_Mutate$, the parent individual does not undergo mutation. Proceed to step ④;

② If $RX \leq P\_Mutate$, the parent individual undergoes mutation. After scaling and binary encoding, a random location on the binary gene fragment is selected for mutation. If the selected location is originally 0, it changes to 1; otherwise, it becomes 0;

③The mutated binary offspring is then decoded and scaled to obtain the target offspring individual. If the parameters of the offspring individual exceed the extreme values, the extreme values will be used instead;

④Repeat steps ①–③ until all the N_{select} individuals have been processed.

Where P_Mutate is the probability of mutation.

Update of population

Using the elite reservation strategy, the optimal individual of the t-th generation, selected based on the fitness function, is copied Nc times ($Nc = (1\text{-}Gap) \times N$). These copies serve as newly generated offspring individuals. The newly generated offspring individuals Nc, along with the offspring individuals N_{select}, form the population of the $(t+1)$-th generation.

Continue iterating until the maximum number of iterations is reached. Then, terminate the iteration process and output the optimal solution.

Where t is the number of the iterations; and Nc is the count of the optimal clones.

Procedure of IRSGA

The procedure of optimizing the parameters for annulus aerated dual gradient drilling using IRSGA is shown in Algorithm 1. The other relevant calculation functions are shown in Algorithms 2 ~ 7.

Algorithm 1 IRSGA for parametersoptimization

```
1: Function IRSGA ():
2: Let t=0, initialize population A_t;
3: Do while t<=T;
4: Evaluate fitness();
5: Selection();
6: Crossover();
7: Mutation();
8: Update population();
9: Let t=t+1;
10: End do;
11: Return best solution.
```

Algorithm 2 Function initialize population for IRSGA

1: Function Initialize population():
2: Create an empty population list A_t;
3: For i=1 to N;
For each individual a_i, randomly generate a chromosome from the search space and add it to the population list A_t;
4: End for;
5: Return the population list A_t.

Algorithm 3 Function evaluate fitness for IRSGA

1: Function Evaluate fitness():
2: Let C_$Fitness_0$=0;
3: For i=1 to N;
4: For each individual a_i, calculate its fitness value $Fitness_i$;
5: Let C_$Fitness_i$= C_$Fitness_{i-1}$+ $Fitness_i$;
5: End for;
6: Return fitness values.

Algorithm 4 Function selection for IRSGA

1: Function Selection():
2: Create an empty parent population list A_{select};
3: For i=1 to N;
4: For each individual a_i, judge whether a_i is selected by the improved selection operator mentioned above, and if so, add a_i to A_{select};
5: End for;
6: Return the population list A_{select}.

Algorithm 5 Function crossover for IRSGA

1: Function Crossover():
2: Randomly sort the individuals in A_{select};
3: For i=2 to N_{select} step 2;
4: For each pair of parent individuals a_{i-1} and a_i, perform the following steps;
5: Generate a random number r and determine if a crossover operation will be performed;
6: Select a crossover point at random from individual;
7: If r is less than the crossover probability, exchange the genes before and after the intersection point of a_{i-1} and a_i;
8: If not, keep a_{i-1} and a_i unchanged;
9: End for;
10: Return the population list A_{select}.

Algorithm 6 Function mutation forIRSGA

1: Function Mutation():
2: For i=1 to N_{select};
3: For each offspring individual a_i, perform the following steps;
4: Generate a random number r and determine if a mutation operation will be performed;
5: If r is less than the mutation probability, randomly select a gene position and perform a mutation operation on the gene at that position;
6: End for;
7: Return the population list A_{select}.

Algorithm 7 Function update population for IRSGA

1: Function Update population():
2: Create an empty parent population list A_{t+1};
3: Let $N_{elitism}$=N-N_{select};
4: Use elitism strategy to generate $N_{elitism}$ individuals and add them to the new population list A_{t+1};
5: Add A_{select} to the new population list A_{t+1};
7: Return the population list A_{t+1}.

Table 2 Wellbore geometry

Name	Hanger depth (m)	Setting depth (m)	Outer diameter (mm)	Wall thickness (mm)
Casing	0	7120	200.03	10.92
Name	Length (m)	Planed well depth (m)	Bit size (mm)	/
Open hole	238	7358	152.4	/

Results and discussion

Case data

The optimization parameters are derived from well FY-X in the Fuyuan block of Tarim Oilfield. The current depth of the well is 7150 m, with a formation pore pressure of 68.3 MPa and a fracture pressure of 71.7 MPa. The drill string consists of a combination of 5-inch dual-wall drill pipe and 3 1/2-inch drill pipe. The annulus channel of the dual-wall drill pipe is utilized as a gas injection pipeline. The density of the drilling fluid is 1200 kg/m^3. Please refer to Table 2 for further details on the wellbore structure.

According to the technological requirements of annulus aerated dual gradient drilling, the parameters must adhere to specific constraints, outlined in Table 3:

The involved computing environment is Inter Core TM i7–1165G7 running Windows 10 with 2.80-GHz processor and 16.00-GB RAM. The experiments are developed by C#.

Table 3 Constraints on parameters

Number	Parameter	Lower limit	Upper limit	Unit
1	Drilling fluid flow rate	5	15	$10^{-3}\times m^3/s$
2	Gas injection flow rate	20	80	$60^{-1}\times m^3/s$
3	Dual-wall drill pipe depth	200	2500	m
4	Wellhead back pressure	0.1	1	$10^6\times Pa$

Results of IRSGA optimization

This article conducts multi-objective optimization of the parameters for annulus aerated dual gradient drilling utilizing the IRSGA. The parameters involved in the genetic algorithm are provided in Table 4.

Table 4 Parameters involved in IRSGA

Number	Parameter	Value
1	Population size	100
2	Number of iterations	100
3	Cross probability	0.8
4	Mutation probability	0.02
5	Generation gap	0.9

Figure 4 shows the variation of population fitness and average fitness with the increase in iteration steps in the IRSGA process of the parameters optimization for annulus aerated dual gradient drilling. The larger the fitness value, the better the individual is, representing a safer and lower cost wellbore. The average fitness value represents the degree of evolution of the population. From Fig. 4, it can be observed that starting from the 30th generation, the population tends to converge. Afterward, the minor fluctuations in the average fitness values represent mutations generated by a small number of individuals during the iteration process, which helps enhance exploration of the solution space. Figures 5 and 6 depict the variations in the bottom-hole pressure and cost coefficient under the optimal parameter combinations for each generation during the IRSGA optimization process. It can be seen that the final bottom-hole pressure

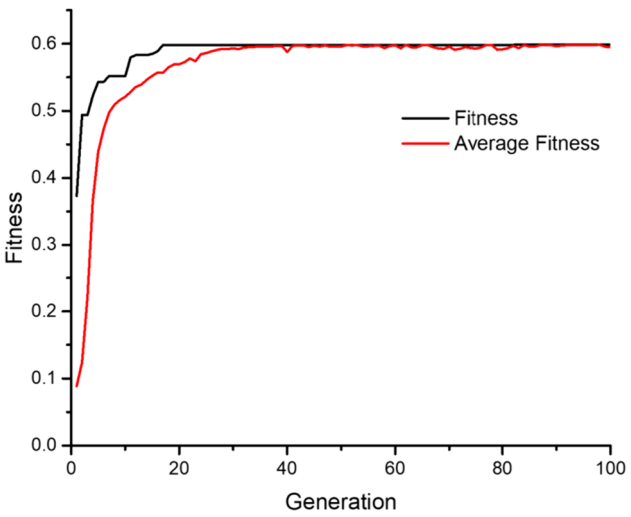

Fig. 4 The variation curve of the fitness and average fitness values with increasing iteration

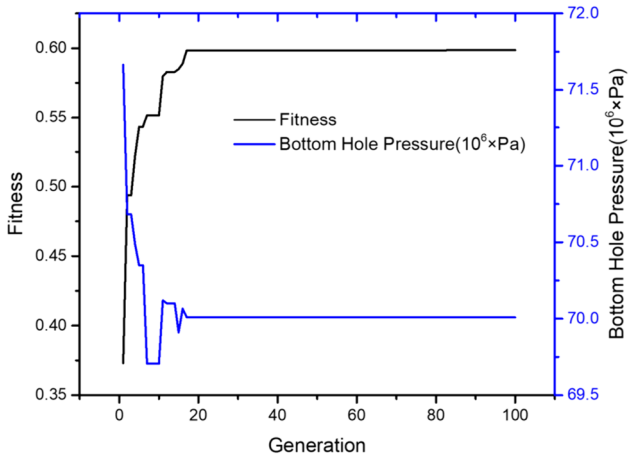

Fig. 5 The variation curve of the bottom-hole pressure with increasing iteration

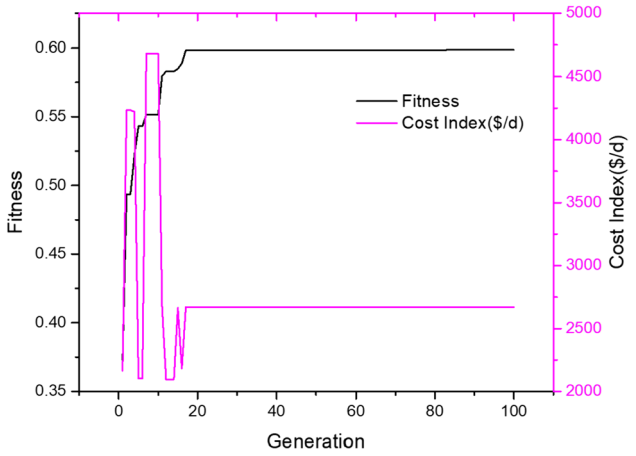

Fig. 6 The variation curve of the cost index with increasing iteration

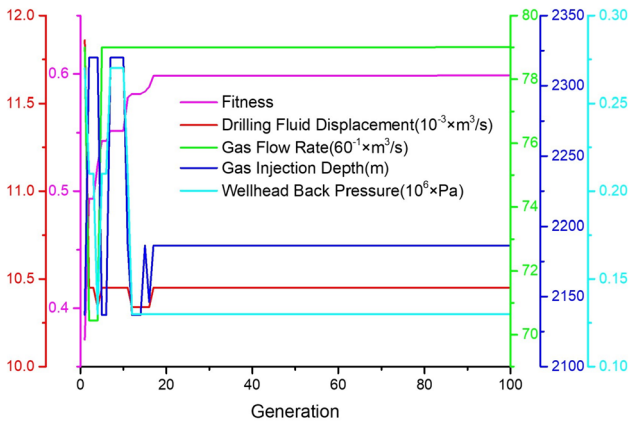

Fig. 7 The variations of the optimal parameter combinations during the IRSGA process

stabilizes at 70 MPa, and the cost coefficient stabilizes at 2670.99 $/d.

Figure 7 represents the variations of the optimal parameter combinations for each generation during the IRSGA optimization process. It is obvious that before the 20th generation, the optimal parameter combinations keep evolving. However, after that, the algorithm converges, and the optimal parameter combinations stabilize without further changes. Therefore, the final optimized parameters are obtained, which ensure that the bottom-hole pressure in the drilling process remains within the safe pressure window while minimizing the construction cost. Compared with the parameters designed with the empirical gas–liquid ratio method (Liu 2022), the cost coefficient is reduced by 36.46%. The detailed results are shown in Table 5.

Results of comparison

Comparison of different genetic algorithms

In this study, we conducted a comparative analysis of the parameter optimization results of the IRSGA with ORSGA, RSGA, and TSGA. We evaluated the on-line and off-line performance and analyzed the impact of different selection operators on the optimization performance of genetic algorithms. The relevant parameters are shown in Table 6. Twenty simulations were conducted for each of the four genetic algorithms mentioned above. The optimization results are shown in Table 7.

John Holland (2013) proposed on-line performance and off-line performance to evaluate the performance of genetic algorithms.

(1) The on-line performance $P_{\text{on-line}}$:

$$P_{\text{on - line}} = \frac{1}{T}\sum_{t=1}^{T}\left(\frac{1}{N}\sum_{i=1}^{N} f(a_i,t)\right) \tag{18}$$

The on-line performance represents the changes in the average fitness value of the population, mainly describing the overall performance and evolutionary ability of the population.

(2) The off-line performance $P_{\text{off-line}}$:

$$P_{\text{off - line}} = \frac{1}{T}\sum_{i=1}^{T} f^{*}(a_i,t) \tag{19}$$

The off-line performance represents the changes in the fitness values of the best individual in the population, mainly describing the individual's evolutionary ability.

$$f^{*}(a_i,t) = \max\left\{f(a_1,t), f(a_2,t) \ldots\ldots, f(a_N,t)\right\} \tag{20}$$

Table 5 Comparison of optimization results for IRSGA

Name	Drilling fluid flow rate ($10^{-3}\times m^3/s$)	Gas injection rate ($60^{-1}\times m^3/s$)	Dual-wall drill pipe depth (m)	Wellhead back pressure ($10^6\times Pa$)	Bottom-hole pressure ($10^6\times Pa$)	Cost index ($/d)
IRSGA method	10.45	79.01	2186.47	0.13	70.01	2670.99
Gas–liquid ratio method	13	80	3000	0.3	70.13	4203.71

Table 6 Parameters of the genetic algorithm

Number	Parameter	Value
1	Population size	40
2	Number of iterations	50
3	Cross probability	0.8
4	Mutation probability	0.02
5	Generation gap	0.9

where $f^*(a_i,t)$ is the best individual fitness value in the current population.

In the experiment, Figs. 8 and 9 compared the $P_{on\text{-}line}$ and $P_{off\text{-}line}$ for the four different genetic algorithms. From the graphs, we can analyze the following points: (1) The selection operator has a significant impact on the performance of genetic algorithms. Improving the selection operator can enhance the algorithm's performance. (2) IRSGA demonstrates good performance in both searching for the optimal individual and the overall evolution of the population. It is first quartile, median and third quartile of $P_{on\text{-}line}$ and $P_{off\text{-}line}$ are larger compared to the other algorithms. Additionally, the interquartile range is smaller, indicating a smaller fluctuation range. (3) RSGA and TSGA yield similar results. However, when the population size is larger, RSGA requires more computational resources for sorting operations.

Comparison of different optimization algorithms

A comparative analysis was conducted between the IRSGA and the PSO (Iweh and Akupan 2023) as well as the SAA (Uday Sankar et al. 2023). The comparative experiments covered both small-scale and large-scale instances. The population size was set to 100 for the small-scale instances and 200 for the large-scale instances. Tables 8 and 9 present the optimization results of fitness function values for small-scale and large-scale instances in the IRSGA, PSO algorithm, and SAA. The "Fitness" and "Ave Fitness" represent the final fitness value and the average fitness value for each instance. Table 10 shows the optimization computation time for small-scale and large-scale instances of IRSGA, PSO, and SAA. The astringency of the instance is determined by Eq. (21). Instances that satisfy Eq. (21) are considered globally convergent, denoted as $GC=1$. Otherwise, they are considered locally convergent, denoted as $LC=1$. The accuracy evaluation of the algorithms is performed based on Eq. (22), and the results are presented in Table 11.

$$\left|\frac{\text{Fitness}_{ij}-\text{Max\_Fitness}}{\text{Max\_Fitness}}\right|\le\varepsilon \tag{21}$$

where Fitness_{ij} refers to the fitness value for the j-th algorithm in the i-th case. Max_Fitness is the limit of the fitness function value. Max_Fitness = 0.6; $\varepsilon=0.01$.

$$AR_j=\frac{m-\sum_{i=1}^{m}LC_{IJ}}{m}\times 100\% \tag{22}$$

where AR_j is the accuracy rate of the j-th algorithm. The m represents the number of algorithm runs, with $m=20$. LC_{ij} denotes the local convergence of the optimization algorithm, while GC_{ij} represents the global convergence.

Table 7 Optimization results of the four genetic algorithms

Method	Evaluating indicator	Max	Min	Average	Square deviation	Standard deviation
ORSGA	Off-line performance	0.562487	0.266983	0.487149	0.005363	0.073235
	On-line performance	0.501347	0.215951	0.413272	0.003857	0.062105
RSGA	Off-line performance	0.596776	0.427983	0.525525	0.002383	0.048816
	On-line performance	0.593431	0.375766	0.479413	0.002965	0.054450
TSGA	Off-line performance	0.583491	0.344837	0.521823	0.003677	0.060635
	On-line performance	0.566054	0.298546	0.462996	0.003913	0.062552
IRSGA	Off-line performance	0.596929	0.519960	0.557872	0.000522	0.022840
	On-line performance	0.594166	0.471065	0.516717	0.001045	0.032329

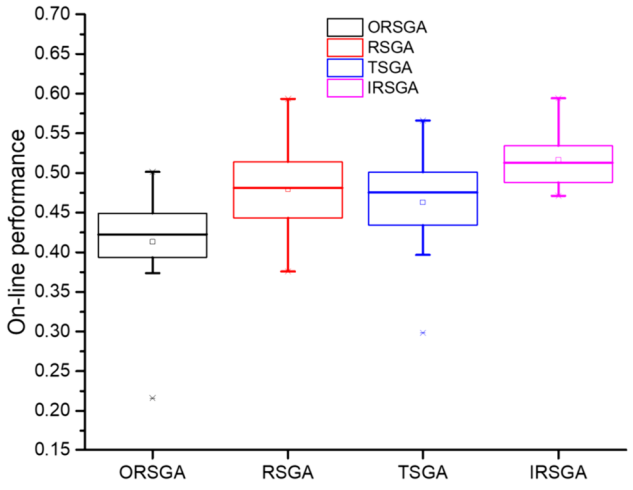

Fig. 8 Box plot of different genetic algorithms about on-line performance

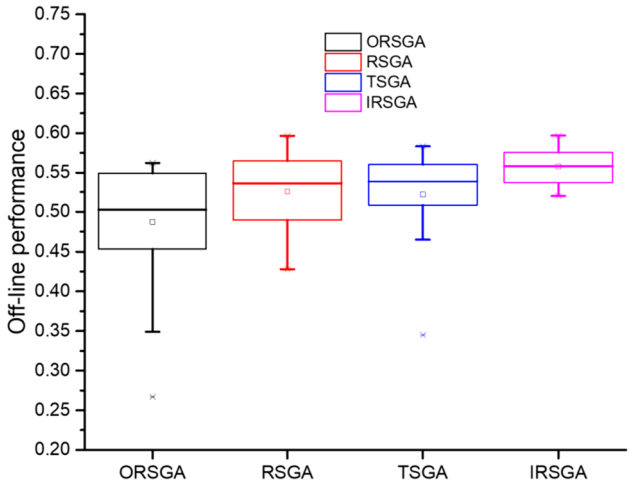

Fig. 9 Box plot of different genetic algorithms about off-line performance

Tables 8 and 9 show that the IRSGA demonstrates good effectiveness and stability in terms of fitness value and average fitness value. Table 10 shows the computation time of each algorithm for both small- and large-scale instances. For small-scale instances, the average computation time for IRSGA optimization is 245.93 s, while for PSO, it is 209.03 s, and for SAA, it is 806.90 s. For large-scale instances, the average computation time for IRSGA optimization is 502.65 s, for PSO, it is 419.22 s, and for SAA, it is 1609.42 s. There is little difference in computational efficiency between IRSGA and PSO, while SAA exhibits the lowest computational efficiency. In terms of accuracy, the IRSGA achieves the highest optimization accuracy. For small-scale instances, the *AR* of IRSGA is 90%, while for large-scale instances, it increases to 95%. In conclusion, the IRSGA proposed in this paper demonstrates excellent performance in terms of solution effectiveness, computational efficiency, and algorithm accuracy.

On-line and off-line evaluation between IRSGA and PSO

As a result of the low computational efficiency of the SAA, further discussion was abandoned. Instead, we conducted the on-line and off-line performance evaluation of the PSO algorithm and IRSGA. The on-line and off-line performance for the optimization results of both algorithms are shown in Table 12. Furthermore, a comparison of the on-line and off-line performance is presented in Table 13.

In terms of on-line performance, the median and third quartile values of PSO and IRSGA are relatively similar. However, the minimum and first quartile values of PSO are significantly smaller than those of IRSGA, as illustrated in Fig. 10. This indicates that the overall evolutionary performance of the IRSGA is superior to that of PSO. Regarding off-line performance, the maximum and third quartile values of PSO are approximate to those of IRSGA. Surprisingly, even the median value of PSO is slightly larger. However, the minimum and first quartile values of PSO are considerably smaller than those of IRSGA. Consequently, the individual evolution performance of the PSO algorithm is inferior to that of IRSGA. In summary, the IRSGA excels in both individual and overall evolution, demonstrating smaller evolutionary fluctuations and greater stability.

Conclusions and future works

In this paper, we proposed a new genetic algorithm-based optimization method called IRSGA for the parameters optimization of annulus aerated dual gradient drilling. We conducted a comprehensive comparative analysis and evaluation on the optimization performance of this algorithm, leading to the following conclusions:

(1) The IRSGA offers distinct advantages in maintaining bottom-hole pressure within the safe pressure window and simultaneously reducing drilling costs. Compared to traditional gas–liquid ratio parameter design methods, the implementation of the IRSGA can result in a substantial cost reduction of 36.46%.
(2) Improving the selection operator can significantly enhance the performance of genetic algorithms. In comparison with ORSGA, RSGA, and TSGA, the IRSGA proposed in this paper demonstrates better convergence and stability.

Table 8 The optimization results for small-scale instances of IRSGA, PSO, and SAA

Case	IRSGA		PSO		SAA	
	Fitness	Ave fitness	Fitness	Ave fitness	Fitness	Ave fitness
1	0.599664	0.583899	0.599834	0.597714	0.597115	0.592185
2	0.598134	0.595384	0.599039	0.594892	0.597229	0.584805
3	0.595613	0.581316	0.425102	0.424102	0.595974	0.589946
4	0.598647	0.588102	0.599491	0.596908	0.597375	0.592061
5	0.599839	0.583796	0.599834	0.596720	0.457652	0.422661
6	0.598982	0.597941	0.599834	0.596921	0.597931	0.582307
7	0.545464	0.513522	0.594198	0.583313	0.595866	0.587847
8	0.596929	0.595110	0.595566	0.588462	0.494673	0.458253
9	0.598992	0.590992	0.425102	0.415102	0.596143	0.585084
10	0.599839	0.596054	0.598294	0.594025	0.597419	0.592878
11	0.596081	0.586156	0.599302	0.598234	0.594783	0.586137
12	0.597953	0.597478	0.431306	0.431046	0.409722	0.373132
13	0.599664	0.584626	0.599834	0.587595	0.593928	0.589809
14	0.596173	0.590204	0.599482	0.587595	0.591005	0.587927
15	0.599836	0.585681	0.598978	0.574517	0.396519	0.356674
16	0.599492	0.599232	0.598636	0.589686	0.597331	0.590628
17	0.598465	0.596609	0.454995	0.435012	0.596335	0.584073
18	0.476481	0.470603	0.597967	0.587381	0.516207	0.490121
19	0.597621	0.593784	0.597604	0.590003	0.595328	0.581846
20	0.596996	0.590032	0.596741	0.577442	0.599704	0.582916

Table 9 The optimization results for large-scale instances of IRSGA, PSO, and SAA

Case	IRSGA		PSO		SAA	
	Fitness	Ave fitness	Fitness	Ave fitness	Fitness	Ave fitness
1	0.597189	0.595162	0.597021	0.587136	0.495502	0.469049
2	0.598041	0.588815	0.596803	0.588863	0.595255	0.589825
3	0.595493	0.588467	0.597492	0.592968	0.597534	0.591327
4	0.595843	0.586132	0.596086	0.589237	0.595801	0.593423
5	0.599873	0.598546	0.423991	0.401139	0.599751	0.592146
6	0.597629	0.594336	0.599821	0.596263	0.408594	0.385851
7	0.596467	0.588063	0.599836	0.596906	0.598814	0.592483
8	0.597788	0.596527	0.596884	0.594882	0.595965	0.589493
9	0.596762	0.593971	0.595308	0.592455	0.596646	0.593019
10	0.596909	0.588794	0.598251	0.594321	0.595328	0.585238
11	0.595438	0.586911	0.435957	0.415888	0.598028	0.588668
12	0.595396	0.594094	0.599364	0.598115	0.595637	0.584875
13	0.496224	0.458651	0.599865	0.591675	0.526349	0.490544
14	0.597589	0.592871	0.598684	0.587978	0.599929	0.597818
15	0.598455	0.592337	0.596857	0.586530	0.596661	0.588282
16	0.599667	0.591816	0.597939	0.591559	0.598307	0.588738
17	0.598448	0.596709	0.597959	0.594495	0.597945	0.594884
18	0.599622	0.593625	0.542562	0.519628	0.599749	0.593228
19	0.599815	0.589988	0.597781	0.589986	0.449699	0.429584
20	0.597422	0.593138	0.598146	0.592974	0.596995	0.587272

Table 10 The optimization time of IRSGA, PSO, and SAA

Case	Small-scale			Large-scale		
	IRSGA	PSO	SAA	IRSGA	PSO	SAA
	Ts(s)	Ts(s)	Ts(s)	Ts(s)	Ts(s)	Ts(s)
1	240.50	195.55	822.83	519.50	418.33	1634.17
2	253.59	203.50	794.23	521.72	416.59	1619.77
3	242.64	226.91	827.73	512.53	407.58	1603.40
4	227.73	210.73	799.00	474.14	418.56	1559.12
5	253.47	212.59	785.93	521.92	426.95	1605.05
6	256.24	196.58	826.78	485.77	429.37	1596.30
7	258.14	203.78	759.78	516.66	431.46	1653.71
8	228.40	206.02	816.48	521.12	430.85	1560.97
9	259.74	205.42	812.95	507.56	427.65	1643.97
10	235.24	212.30	762.36	478.40	437.24	1633.88
11	247.34	207.58	814.37	506.47	425.28	1687.30
12	260.83	223.71	856.18	501.08	407.20	1607.63
13	236.86	214.05	801.08	535.87	410.61	1606.25
14	258.11	201.93	778.54	477.60	403.22	1565.59
15	235.37	215.21	846.97	470.89	417.62	1645.12
16	230.56	203.38	797.06	495.31	421.28	1592.34
17	249.68	216.58	848.94	469.05	401.27	1675.61
18	245.76	216.05	748.53	530.75	420.07	1520.46
19	242.21	203.21	767.62	476.09	426.91	1592.11
20	256.19	205.52	870.72	530.58	406.37	1585.58

Table 11 The optimization astringency and accuracy results of IRSGA, PSO, and SAA

Case	Small-scale						Large-scale					
	IRSGA		PSO		SAA		IRSGA		PSO		SAA	
	GC	LC	GC	LC	GC	LC	GC	LC	GC	LC	GC	LC
1	1	0	1	0	1	0	1	0	1	0	0	1
2	1	0	1	0	1	0	1	0	1	0	1	0
3	1	0	0	1	1	0	1	0	1	0	1	0
4	1	0	1	0	1	0	1	0	1	0	1	0
5	1	0	1	0	0	1	1	0	0	1	1	0
6	1	0	1	0	1	0	1	0	1	0	0	1
7	0	1	1	0	1	0	1	0	1	0	1	0
8	1	0	1	0	0	1	1	0	1	0	1	0
9	1	0	0	1	1	0	1	0	1	0	1	0
10	1	0	1	0	1	0	1	0	1	0	1	0
11	1	0	1	0	1	0	1	0	0	1	1	0
12	1	0	0	1	0	1	1	0	1	0	1	0
13	1	0	1	0	1	0	0	1	1	0	0	1
14	1	0	1	0	1	0	1	0	1	0	1	0
15	1	0	1	0	0	1	1	0	1	0	1	0
16	1	0	1	0	1	0	1	0	1	0	1	0
17	1	0	0	1	1	0	1	0	1	0	1	0
18	0	1	1	0	0	1	1	0	0	1	1	0
19	1	0	1	0	1	0	1	0	1	0	0	1
20	1	0	1	0	1	0	1	0	1	0	1	0
Sum	18	2	16	4	15	5	19	1	17	3	16	4
AR	90%		80%		75%		95%		85%		80%	

Table 12 Optimization results of on-line performance and off-line performance

PSO		IRSGA	
On-line performance	Off-line performance	On-line performance	Off-line performance
0.473586	0.574815	0.520004	0.565815
0.498939	0.555064	0.505025	0.546663
0.576307	0.578931	0.528933	0.571739
0.530406	0.575762	0.490584	0.532977
0.503722	0.576307	0.531037	0.572701
0.414036	0.418382	0.482386	0.534913
0.408843	0.421763	0.584886	0.596929
0.349373	0.354953	0.594166	0.594546
0.548016	0.586252	0.485122	0.531261
0.553116	0.582704	0.485722	0.538745
0.512661	0.579777	0.506064	0.551333
0.419812	0.429675	0.533322	0.575811
0.495088	0.520823	0.535456	0.575049
0.488816	0.588135	0.534815	0.576210
0.522923	0.589706	0.535473	0.578398
0.482331	0.514347	0.474848	0.520109
0.532617	0.576751	0.503503	0.550917
0.533315	0.578657	0.471065	0.519960
0.533442	0.562195	0.531827	0.575525
0.357855	0.363675	0.500098	0.547841

Table 13 Comparison results of on-line performance and off-line performance

Method	Evaluating indicator	Max	Min	Average	Square deviation	Standard deviation
PSO	Off-line performance	0.589706	0.354953	0.526434	0.006142	0.078372
	On-line performance	0.576307	0.349373	0.486760	0.003927	0.062667
IRSGA	Off-line performance	0.596929	0.519960	0.557872	0.000522	0.022840
	On-line performance	0.594166	0.471065	0.516717	0.001045	0.032329

(3) In terms of optimization stability, efficiency, and computational accuracy, IRSGA performs better than PSO and SAA, especially in large-scale computations, where its computational accuracy exceeds 95%.
(4) On the aspect of on-line and off-line performance, the IRSGA performs better than the PSO algorithm.

However, there are still limitations and areas for improvement in this study. Local optima have not been entirely avoided, and there is a need to enhance computational efficiency. Moving forward, there are several directions for future research. Firstly, it would be beneficial to further explore the impact of population size on convergence ability. Additionally, improvements can be made to the crossover and mutation operations in order to enhance the algorithm's global exploration ability. Lastly, it is significative

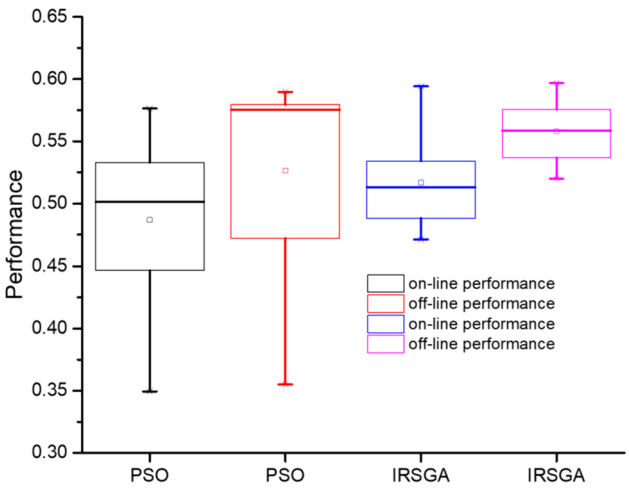

Fig. 10 Box plot of PSO and IRSGA about on-line and off-line performance

to investigate the influence of population renewal strategies on the overall performance of the algorithm.

Author contributions Qian Li, Xiaolin Zhang, and Hu Yin helped in conceptualization; Xiaolin Zhang helped in methodology; Xiaolin Zhang worked in software; Xiaolin Zhang, Qian Li, and Hu Yin helped in validation; Xiaolin Zhang helped in formal analysis; Qian Li worked in investigation; Qian Li helped in resources; Xiaolin Zhang contributed to writing—original draft preparation; Xiaolin Zhang contributed to writing—review and editing; Hu Yin and Xiaolin Zhang worked in supervision; Qian Li worked in project administration; and Qian Li helped in funding acquisition. All authors have read and agreed to the published version of the manuscript.

Funding This work was supported by the China National Key Research and Development Project (2019YFA0708302).

Data availability Not applicable.

Declarations

Conflict of interest The authors declare no conflict of interest.

Institutional review board statement Not applicable.

Informed consent statement Not applicable.

References

Chande SV, Sinha M (2013) Genetic algorithm: a versatile optimization tool. Bvicams Int J Inf Technol 1:7–13

Dou L, Li G, Shen Z, Wu C, Liu W (2013) Technological design and parametric analysis of annular aerated drilling. China Petrol Mach 41(2):14–19

Gonzalez F, Franco R, Rodriguez R, Gamez G, Blas B, Vasquez J, Alcudia H (2013) Successful application of concentric casing nitrogen injection to overcome drilling challenges and deliver a record horizontal well in the tecominoacan field. In: SPE/IADC drilling conference: Amsterdam, The Netherlands. https://doi.org/10.2118/163494-MS

Guo B, Rajtar JM (1995) Volume requirements for aerated mud drilling. Spe Drill Complet 10(3):165–169. https://doi.org/10.2118/26956-PA

Hasan AR, Kabir CS (1986) A Study of multiphase flow behavior in vertical oil wells: Part I - theoretical treatment. In: SPE California regional meeting. society of petroleum engineers: Oakland, California.

Holland J (2013) Adaptation in natural and artificial systems: an introductory analysis with applications to biology, control, and artificial intelligence. University of Michigan Press, Ann Arbor

Iweh CD, Akupan ER (2023) Control and optimization of a hybrid solar PV–hydro power system for off-grid applications using particle swarm optimization (PSO) and differential evolution (DE). Energy Rep 10:4253–4270. https://doi.org/10.1016/j.egyr.2023.10.080

Li Y (2007) The low pressure drilling technique with dual-wall drill-pipe. Petrol Drill Tech 35(2):1–4

Liu R (2022) Study on gas production technology of suction and gas lift drainage, Dissertation Northeast Petroleum University

Lopes CA, Jr. Bourgoyne AT (1997) Feasibility study of a dual density mud system for deepwater drilling operations. In: offshore technology conference: Houston, Texas. https://doi.org/10.4043/8465-MS

Ma Y, Sun B, Shao R, Wang Z, Liu X (2014) Simulation computation of temperature field in riser annulus for dual-gradient drilling using gas injection. Acta Petrolei Sinica 35(4):779–785

Mao F, Ma L, He Q, Xiao G (2020) Match making in complex social networks. Appl Math Comput 371:124928. https://doi.org/10.1016/j.amc.2019.124928

Meng Y, Xu C, Wei N, Li G, Li H, Duan M (2015) Numerical simulation and experiment of the annular pressure variation caused by gas kick/injection in wells. J NAT GAS SCI ENG 22:646–655. https://doi.org/10.1016/j.jngse.2015.01.013

Ong JY, King YJ, Saw LH, Theng KK (2019) Optimization of the design parameter for standing wave thermoacoustic refrigerator using genetic algorithm. In: IOP conference series: earth and environmental science: Kuala Lumpur, Malaysia. https://doi.org/10.1088/1755-1315/268/1/012021/pdf

Pandey HM (2016) Performance evaluation of selection methods of genetic algorithm and network security concerns. Proced Comput Sci 78:13–18. https://doi.org/10.1016/j.procs.2016.02.004

Stave R, Fossli B, Endresen C, Rezk RH, Tingvoll GI, Thorkildsen M (2014) Exploration drilling with riserless dual gradient technology in arctic waters. In: OTC arctic technology conference: Houston, Texas. https://doi.org/10.4043/24588-MS

Su P, Li S, Li L, Wan X, Chen Y (2018) Experimental study on gas migration process in riser for dual gradient drilling. China Petrol Mach 46(1):16–20

Sun J, Bai Y, Cheng R, Lyu K, Liu F, Feng J, Lei S, Zhang J, Hao H (2021) Research progress and prospect of plugging technologies for fractured formation with severe lost circulation. Petrol Explor Dev 48(3):732–743. https://doi.org/10.1016/S1876-3804(21)60059-9

Uday Sankar K, Bhasi M, Madhu G (2023) A hybrid bacterial foraging–simulated annealing framework for improving road networks. Meas Sens 26:100704

Wang J, Li J, Liu G, Huang T, Yang H (2019) Parameters optimization in deepwater dual-gradient drilling based on downhole separation. Petrol Explor Dev 46(4):819–825. https://doi.org/10.1016/s1876-3804(19)60240-5

Westermark RV (1986) Drilling with a parasite aerating string in the disturbed belt, gallatin county, montana. In: IADC/SPE drilling conference: Dallas, Texas. https://doi.org/10.2118/14734-MS

Yang H, Li J, Zhang G, Zhang H, Guo B, Chen W (2022) Wellbore multiphase flow behaviors during gas invasion in deepwater downhole dual-gradient drilling based on oil-based drilling fluid. Energy Rep 8:2843–2858. https://doi.org/10.1016/j.egyr.2022.01.244

Zimuzor MO, Shannon MH, Goke A, Tom RB, Ricardo JA, Danny B (2010) Managed-pressure drilling using a parasite aerating string. Spe Drill Completion 25(4):564–576. https://doi.org/10.2118/119964-pa